

Quantum-to-classical correspondence in Krylov complexity

Gastón F. Scialchi,^{1,2,*} Augusto J. Roncaglia,^{1,2} and Diego A. Wisniacki^{1,2,†}

¹*Universidad de Buenos Aires, Facultad de Ciencias Exactas y Naturales, Departamento de Física. Buenos Aires 1428, Argentina*

²*CONICET - Universidad de Buenos Aires, Instituto de Física de Buenos Aires (IFIBA). Buenos Aires 1428, Argentina*

We study quantum-to-classical correspondence of the Krylov space for evolutions driven by unitary maps with a classical limit. This entails a proper definition of corresponding quantum and classical operators, inner products and initial states. We prove that with these definitions the purely classical Krylov space is indeed obtained as the asymptotic $\hbar \rightarrow 0$ expansion of the quantum Krylov space, and provide several examples of such correspondence. We use these examples to analyze some general aspects about the evolution of the Krylov complexity as they relate to the phase-space representation for the Krylov states. Additionally, we discuss alternative definitions to obtain the correspondence and why they fail. This paper constitutes a first step in understanding complexity and ergodicity of unitary evolution through the Krylov perspective as they relate to classical dynamical notions.

I. INTRODUCTION

In its inception, the field of quantum chaos was concerned with manifestations of the underlying classically chaotic dynamics in the quantum regime. Many quantities have been studied whose behavior bring to light such manifestations. One example is the relationship between the spectral statistics of a quantum system, such as level and eigenstate statistics, and the chaoticity of its underlying classical counterpart [1–7]. This statistical approach probes global and time-independent properties of the system. A complementary dynamical picture has also been developed, where the focus is on the study of time-dependent quantities whose behavior show signatures of the related classical dynamics. Examples of these quantities are the Loschmidt echo [8, 9], as a probe of the sensitivity to perturbations in the time-reversed evolution of a system, and the out-of-time-order correlator (OTOC), whose growth is associated with the spread of quantum information [10] and has also been related with the Lyapunov exponent if an underlying classical system is present [11–13]. In quantum systems where a classical limit may not exist, its chaoticity is *defined* according to how the aforementioned quantities behave.

Krylov complexity is a recent entry in the dictionary of dynamical quantum chaos. Its original formulation arises in the context of operator growth, where an initially “simple” operator becomes increasingly “complex” as it evolves in the Heisenberg picture, in the sense that it requires an increasing amount of elements from a reference operator basis to construct it, in this case the Krylov basis. A “universal operator growth hypothesis” implies that under chaotic Hamiltonian dynamics Krylov complexity grows exponentially with a rate that upper-bounds that of other operator growth measures such as the OTOC [14], which itself reflects aspects of the underlying classical dynamics (if it exists) as its growth-rate is

related to the Lyapunov exponent, like mentioned above. Under general unitary quantum dynamics, where there may not exist an underlying static Hamiltonian driving the evolution, a complementary picture has been proposed: for chaotic systems, the presence of a “maximally ergodic regime” is a universal feature which in turn implies maximal growth of Krylov complexity [15].

Although the Krylov picture for Hamiltonian dynamics has long been applied equally in both quantum and classical settings, it was mostly used as a tool to probe close-to-equilibrium properties from the dynamics of many-body systems through the recursion method [16]. It is also worth noting that the universal operator growth hypothesis was proposed *including* purely classical dynamics. However, most of the effort since has been focused on the study of systems in the quantum or semiclassical regime.

The aim of this line of work is to establish an understanding on the notions of integrability and chaos as viewed from the Krylov perspective in terms of classical dynamical concepts. As a first step, it is necessary to understand how to correctly define the construction of both a quantum and a classical Krylov space such that they obey the correspondence principle. This is the particular goal of this paper, with a focus in evolutions described by general unitary (super)operators. More precisely, we proved that under suitable choices of inner products and initial states, the resulting Krylov spaces for the quantum evolution of a density matrix and the classical evolution of a probability distribution in phase space, respectively, become identical in the classical limit. We do this by considering a phase space representation of the quantum Krylov states through quasiprobability distributions, and showing that in the limit $\hbar \rightarrow 0$ these distributions match the classical ones exactly. Additionally, we found that an alternative approach to obtain the classical Krylov space in correspondence with a given quantum one based on choosing an initial classical distribution that matches the quasiprobability distribution of the initial quantum state does not work.

The paper is structured as follows. In Sec. II A we review the construction of Krylov space for unitary evo-

* E-mail address: gscialchi@df.uba.ar

† E-mail address: wisniacki@df.uba.ar

lution through the Arnoldi iteration, and define both the quantum and classical Krylov spaces and the Krylov complexity. We then show in Sec. II B that these definitions obey a quantum-to-classical correspondence through a phase-space representation via a quasiprobability distribution. In Appendix C we additionally study an alternative approach to correspondence: to match the classical distribution to that of the phase-space representation for the quantum system, and discuss why it fails. Examples of the correspondence in action are shown in Sec. III, where we compare the Krylov spaces and complexity through the quantum-to-classical transition in quantum models with their purely classical counterparts, with both linear and non-linear dynamics. These examples also serve to interpret general aspects of Krylov space in terms of the phase-space picture. We conclude in Sec. IV with a summary and some final remarks.

II. QUANTUM AND CLASSICAL KRYLOV SPACE

A. Arnoldi iteration construction

Both quantum and classical dynamics can be formulated in terms of an operator \mathcal{U} that propagates an “observable” ρ_0 forwards in time, which in a quantum setting refers to a hermitian operator acting on a Hilbert space and classically to a function defined in phase space. This fact means that in both cases the Krylov space can be constructed much the same way: by considering the repeated applications of the propagator and obtaining an orthonormal basis for the space that it spans (the Krylov basis). This requires the definition of an inner product that determines what “orthonormal” means, and a procedure to construct the aforementioned basis, the Arnoldi iteration is one such procedure that we detail below.

In both quantum and classical dynamics, start with an initial observable ρ_0 and a propagator \mathcal{U} that evolves it in one time step $\rho_t = \mathcal{U}\rho_{t-1}$, where $\rho_t = \mathcal{U}^t\rho_0$ with $t \in \mathbb{N}_0$. Define an inner product $(\cdot|\cdot)$ and induced norm $\|\cdot\| = \sqrt{(\cdot|\cdot)}$. Then, let $\kappa_0 \equiv \rho_0/\|\rho_0\|$ be the first element of the Krylov basis; the rest is obtained recursively by the Arnoldi iteration

$$b_n\kappa_n = \mathcal{U}\kappa_{n-1} - \sum_{l=0}^{n-1} (\kappa_l|\mathcal{U}\kappa_{n-1})\kappa_l, \quad (1)$$

yielding the Krylov basis $\{\kappa_0, \kappa_1, \dots\}$ with $(\kappa_n|\kappa_m) = \delta_{nm}$. The exact same basis can be obtained by applying a Gram-Schmidt orthonormalization directly to the sequence $\{\rho_0, \rho_1, \dots\}$ as detailed in Appendix A. This alternative is useful when one doesn’t have explicit access to the propagator \mathcal{U} itself, but only to the aforementioned sequence, as will be the case in the classical setting. As a practical note, we carry out the orthonormalization step twice (a modification usually referred to as “reorthonormalization”), be it in the Arnoldi iteration or the Gram-

Schmidt procedure. This mitigates the possible loss of orthogonality in the resulting basis as a consequence of finite-precision numerics.

In the resulting Krylov basis, the propagator is represented by a matrix with an upper Hessenberg form, and is completely parametrized by the Arnoldi sequences [15]

$$b_n = (\kappa_n|\mathcal{U}\kappa_{n-1}), \quad a_n = (\kappa_n|\mathcal{U}\kappa_n), \quad c_n = (\kappa_0|\mathcal{U}\kappa_n). \quad (2)$$

Its lower diagonal is defined by b_n , and the rest of the non-zero elements by

$$\mathcal{U}_{mn} = (\kappa_m|\mathcal{U}\kappa_n) = \frac{a_m}{c_m}c_n \quad \forall m \leq n. \quad (3)$$

One may then expand this basis in terms of the evolution

$$\kappa_n = \sum_{t=0}^n \alpha_{tn} \rho_t, \quad (4)$$

or conversely

$$\rho_t = \sum_{n=0}^t \beta_{nt} \kappa_n. \quad (5)$$

We refer to the quantity β_{nt} as the *wavefunction* in Krylov space, since the system is mapped to a quasi one-dimensional hopping problem whose evolution is given by

$$\beta_{n\ t+1} = b_n\beta_{n-1\ t} + a_n\beta_{n\ t} + \alpha_{0\ n} \sum_{\nu=0}^{n-2} c_\nu\beta_{\nu\ t}, \quad (6)$$

where each site on the chain represents a Krylov state. At the first site the wavefunction obeys $\beta_{0\ t} = (\rho_0|\rho_t)/\|\rho_0\|^2$, i.e., it is the normalized autocorrelation.

As stated, the above procedure is completely general and can be applied to any initial observable ρ_0 . Here we are interested in the evolution itself, as such our object of interest is the system’s state. In a quantum setting this means that ρ represents a density matrix and \mathcal{U} is the unitary evolution superoperator. In the case studies of this work, we may define it through $\mathcal{U}\hat{\rho}_t = U\hat{\rho}_{t-1}U^\dagger$, with U being a “usual” unitary evolution operator (from now on we will explicitly denote quantum observables with a hat \hat{A} where sensible). Finally, we define an operator inner product as

$$(\hat{\rho}|\hat{\sigma})_Q = \frac{1}{2\pi\hbar} \text{Tr}(\hat{\rho}^\dagger\hat{\sigma}). \quad (7)$$

In a classical setting, ρ represents a probability distribution over phase space and \mathcal{U} the Perron-Frobenius operator. From now on we will refer to this classical propagator as \mathcal{P} . When associated to a classical area-preserving map \mathcal{M} its action can formally be written as

$$\rho_{t+1}(x) = \mathcal{P}\rho_t(x) = \int dx' \delta(x - \mathcal{M}(x'))\rho_t(x'), \quad (8)$$

where $x = (q, p)$ is a point in phase space. In this case, we use the L^2 inner product

$$(\rho|\sigma)_C = \int dx \rho(x)^* \sigma(x). \quad (9)$$

In practice one may not have access to the Perron-Frobenius operator for the classical evolution. Instead, we evolve the distribution with the associated area-preserving map \mathcal{M} such that $\rho_{t+1}(x) = \rho_t(\mathcal{M}^{-1}(x))$, as Eq. (8) suggests, and apply a Gram-Schmidt orthonormalization procedure to the sequence $\{\rho_0, \rho_1, \dots\}$ as discussed earlier. Interestingly, once finished one can explicitly compute a local matrix representation of the Perron-Frobenius operator by way of Eqs. (3) and (4). It is local because it is reduced to the subspace given by the evolution subject to the initial condition.

Note that, since a density matrix ρ is hermitian (and a probability distribution real), the resulting quantities defined in Krylov space are also all real. However, the space of density matrices (probability distributions) is not closed upon the operations carried on during the construction of Krylov space. This is because the linear combinations that result in (4) are not necessarily convex. Thus, the resulting Krylov states will generally not be density matrices (probability distributions) and will not obey the Kolmogorov axioms.

The procedure above iteratively constructs the minimal Krylov subspace spanning the system evolution up to a given point in time. In both quantum and classical dynamics this framework provides a notion of evolution complexity encapsulated in the Krylov complexity [14, 15, 17]

$$C_{\mathcal{K}}(t) = \sum_{n=0}^t n |\beta_{nt}|^2 \quad (10)$$

as the average dimension of the subspace needed to effectively describe the evolution from its beginning up to a time t . It is important to mention that several definitions of Krylov complexity exist, all with essentially the same expression (10). The ambiguity arises from how the Krylov space is generated: it may be constructed for the Schrödinger evolution of a state (in which case it is also referred to as the “spread complexity” [18, 19]) or the Heisenberg evolution of an operator. Additionally, its behavior also depends on the properties of the (super)operator with which it is expanded. In the present scenario, we are dealing with a unitary superoperator for which the Krylov complexity possesses a linear maximal growth $C_{\mathcal{K}}(t) = t$ that is met when a completely new Krylov state is needed to describe the system’s evolution in each next time step, i.e., $\mathcal{U}\hat{\kappa}_n = \hat{\kappa}_{n+1}$. This also implies that the propagator takes a purely lower diagonal form $(\hat{\kappa}_m|\mathcal{U}\hat{\kappa}_{n-1}) = \delta_{m n+1}$. Such a regime has been referred to as “maximally ergodic” [15].

B. Quantum-to-classical correspondence

In this section we show that the Arnoldi iteration applied to the evolution of a quantum system (with the inner product (7)) has a purely classical counterpart defined by the iteration applied to the evolution a classical distribution in phase space (with the inner product (9)), and that the respective resulting Krylov spaces become equivalent in the classical limit. This equivalence is in the sense that the quasiprobability distributions that represent the quantum Krylov states in phase-space become identical to the purely classical Krylov distributions.

Many phase-space representations through quasiprobability distributions exist and are equivalent, containing the full information of the quantum system’s state. Here we will make use of the Glauber-Sudarshan P-representation [20, 21], which exploits the overcompleteness of the coherent state basis to represent any density matrix in a “diagonal form”

$$\hat{\rho} = \int dx P_{\rho}(x) |\alpha(x)\rangle\langle\alpha(x)|, \quad (11)$$

such that the resulting distribution $P_{\rho}(x)$ is non-negative if the quantum state admits a classical limit [22]. The transformation to obtain this distribution is linear, so Eq. (4) implies that the quantum Krylov states also admit such a representation, although their P-distributions need not be positive as a consequence of the non-convex linear combination.

We will now establish the quantum-to-classical correspondence. Consider the quantum Arnoldi iteration (1) arising from an initial state $\hat{\rho}$ and unitary superoperator \mathcal{U} . By representing its Krylov states in phase space, their P-distributions follow a similar scheme

$$b_n P_{\kappa_n}(x) = P_{\mathcal{U}\kappa_{n-1}}(x) - \sum_{l=0}^{n-1} (\hat{\kappa}_l|\mathcal{U}\hat{\kappa}_{n-1})_Q P_{\kappa_l}(x). \quad (12)$$

On the other hand, consider the classical Krylov space constructed by applying the classical Arnoldi iteration to the initial classical distribution $\rho_0(x) \equiv P_{\rho_0}(x)$ with the propagator \mathcal{P} , that is:

$$b_n \kappa_n(x) = \mathcal{P}\kappa_{n-1}(x) - \sum_{l=0}^{n-1} (\kappa_l|\mathcal{P}\kappa_{n-1})_C \kappa_l(x). \quad (13)$$

This way, since by definition the quantum and classical initial states are identical in phase space, to get (13) from (12) it suffices for the semiclassical quantum evolution to follow the classical, and for the quantum and classical inner products to match in the semiclassical limit [23]. We may express this as the following two conditions:

$$P_{\mathcal{U}\kappa_n}(x) \approx \mathcal{P}\kappa_n(x), \quad (14)$$

$$(\hat{\kappa}_l|\hat{\kappa}_m)_Q \approx (\kappa_l|\kappa_m)_C, \quad (15)$$

where in (14) we are also implicitly requiring that

$$P_{\kappa_n}(x) \approx \kappa_n(x), \quad (16)$$

although this is true on its own provided (14) and (15) hold up to the $(n-1)$ th Krylov state. To show that these conditions indeed hold, we will first need a few related results.

The first result concerns the semiclassical evolution generated by the quantum map. Semiclassically, quantum maps U with a classical counterpart \mathcal{M} evolve coherent states into *squeezed* coherent states centred on the classical trajectory up to an $O(\hbar^{1/2})$ correction [24], which in turn implies that the P-distribution of the evolved state follows

$$P_{U\rho}(x) \approx P_\rho(\mathcal{M}^{-1}(x)) \equiv \mathcal{P}P_\rho(x). \quad (17)$$

The semiclassical propagation of coherent states is treated rigorously in the aforementioned reference, but for clarity we provide in Appendix B an explicit proof of Eq. (17) by direct calculation for a frequently studied type of quantized classical map. Semiclassical correspondence is expected to be valid up to the Ehrenfest time τ_E .

The second result relates the quantum and classical inner products [Eqs. (7) and (9), respectively] through the P-representation (11). By using such a decomposition for any two quantum observables $\hat{\rho}$, $\hat{\sigma}$ and by expressing the trace in the coherent-state basis $\text{Tr}(\hat{A}) = \int dx \langle \alpha(x) | \hat{A} | \alpha(x) \rangle / 2\pi\hbar$, their quantum inner product can be written as

$$\begin{aligned} (\hat{\rho} | \hat{\sigma})_Q &= \iint dy dz P_\rho(y) P_\sigma(z) \frac{1}{2\pi\hbar} e^{-\frac{1}{2\hbar}(z-y)^2} \\ &\approx \int dy P_\rho(y) P_\sigma(y) \equiv (P_\rho | P_\sigma)_C, \end{aligned} \quad (18)$$

where we have first used the closure relation $\int dx |\alpha(x)\rangle\langle\alpha(x)| / 2\pi\hbar = 1$, that the overlap between coherent states is $|\langle\beta(y)|\gamma(z)\rangle|^2 = e^{-\frac{1}{2\hbar}(z-y)^2}$ and that the 0-variance limit of a Gaussian distribution is a Dirac delta. Thus, the quantum inner product of any two observables converges to the *classical* inner product of their P-representations.

Having established these results, we now proceed to show that conditions (14), (15) and (16) hold. Because the classical initial state is defined as $\rho_0(x) \equiv P_{\rho_0}(x)$, Eq. (17) means that $P_{\rho_t}(x) \approx \rho_t(x)$ for times shorter than the Ehrenfest time $t \leq \tau_E$. Then, the inner products of the evolved quantum and classical systems satisfy $(\hat{\rho}_s | \hat{\rho}_t)_Q \approx (\rho_s | \rho_t)_C$ for $s, t \leq \tau_E$ due to Eq. (18). We now proceed iteratively. Starting the iteration (12) at $n = 1$ with $\hat{\kappa}_0 = \hat{\rho}_0 / \|\hat{\rho}_0\|_Q$ we have

$$\begin{aligned} b_1 P_{\kappa_1}(x) &= P_{U\kappa_0}(x) - (\hat{\kappa}_0 | U\hat{\kappa}_0)_Q P_{\kappa_0}(x) \\ &\approx \mathcal{P}\kappa_0(x) - (\kappa_0 | \mathcal{P}\kappa_0)_C \kappa_0(x), \end{aligned}$$

with $\kappa_0(x) = \rho_0(x) / \|\rho_0\|_C$, and where the limit is obtained because conditions (15) and (16) are trivially met for $n = 0$. As a result condition (16) holds for $n = 1$. Because $\hat{\kappa}_1$ is a linear combination of $\hat{\rho}_0$ and $U\hat{\rho}_0$, it also admits an expansion in the P-representation (11) (although

since it isn't a convex sum P_{κ_1} need not be positively defined). Additionally, because of (18), condition (15) also holds for $l, m \leq 1$. This reasoning extends inductively such that these conditions are true up to $l, m, n \leq \tau_E$. This establishes the quantum-to-classical correspondence of the Krylov space through the phase-space representation.

In Appendix C we discuss a seemingly reasonable alternative method to study quantum-to-classical correspondence. Instead of considering a density matrix with the form (11), we take either a pure coherent-state density matrix $|\alpha(x)\rangle\langle\alpha(x)|$ or a ket $|\alpha(x)\rangle$ in the quantum regime and compare with the classical for a Gaussian distribution with variance $\sigma^2 = \hbar$. With this choice, the phase-space-represented quantum distribution and classical distribution of the initial state are identical. Such an approach, where the quantum evolution of some quasiprobability distribution over phase space is compared directly to that of a corresponding classical evolution, has its precedents (for example, Refs. [25–27] to cite a few). Yet, we find that correspondence of the Krylov space is not attained with such method.

III. EXAMPLES

In this section we show the quantum-to-classical transition in Krylov space argued above in a few simple examples and discuss its structure in relation to the representation of the Krylov states in phase space.

While the P-representation is a useful tool for the proof of the previous section, the resulting quasiprobability distribution is not well behaved as the quantum nature of the state is reflected not only in negativities, as with the Wigner distribution, but also with a high degree of singularity. As mentioned, many such representations exist and are equivalent. In particular, throughout the manuscript we will make use of the Husimi distribution [28–30]

$$H_\rho(x) = \frac{1}{2\pi\hbar} \langle \alpha(x) | \hat{\rho} | \alpha(x) \rangle, \quad (19)$$

which amounts to an \hbar -Gaussian smoothing of the P-distribution, making it non-singular.

A. Harmonic oscillator

The simplest case study is the Harmonic oscillator. In this case the quantum-to-classical correspondence argued above holds trivially since the quantum evolution itself maps coherent states onto other coherent states.

For simplicity, we consider the Harmonic oscillator as a map through

$$\begin{aligned} q' &= q + \tau p \\ p' &= p - \tau q', \end{aligned} \quad (20)$$

having set both its frequency and mass to unity. This is a good approximation for small values of τ and sufficient for our purposes. Quantum mechanically we treat it with the usual unitary operator $U = e^{-i\tau(\hat{N} + \frac{1}{2})}$. To construct the initial state we do not calculate the P-representation of a density matrix, but we do the inverse operation: we define the classical distribution $\rho_0(q, p)$ beforehand and utilize a discrete-basis representation of the coherent states to compute $\hat{\rho}$ using Eq. (11) explicitly. In this case, the initial state chosen is defined by a Gaussian distribution centered at a point (q_0, p_0) with variance σ^2 as

$$\rho_0(q, p) = \frac{1}{2\pi\sigma^2} e^{-\frac{1}{2\sigma^2}[(q-q_0)^2 + (p-p_0)^2]}. \quad (21)$$

For its quantum counterpart of the form (11), the Husimi distribution (19) can be easily computed

$$H_{\rho_0}(q, p) = \frac{1}{2\pi(\hbar + \sigma^2)} e^{-\frac{1}{2(\hbar + \sigma^2)}[(q-q_0)^2 + (p-p_0)^2]}, \quad (22)$$

which is simply the distribution arising from the direct composition of the classical (σ) and quantum ($\sqrt{\hbar}$) uncertainties, and explicitly meets $\lim_{\hbar \rightarrow 0} H_{\rho_0}(q, p) = \rho_0(q, p)$. For the calculations that follow we have set $\tau = 0.1$, which sets the periodicity of the oscillator at $T \approx 63$ time steps, and parameters for the initial condition $(q_0, p_0) = (1, 0)$ and $\sigma = 0.1$.

The full picture of the Krylov space and dynamics through the quantum-to-classical transition can be seen in Figs. 1, 2 and 3, showing the Arnoldi sequences, the Krylov complexity and the Krylov states, respectively, for different values of \hbar .

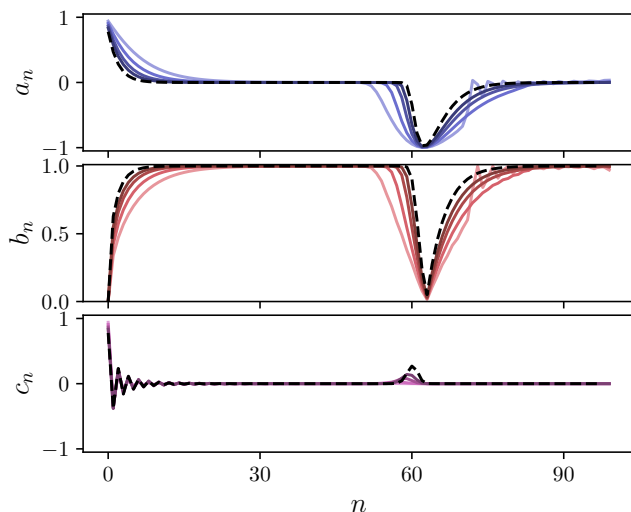


Figure 1. Quantum-to-classical correspondence in the Arnoldi sequences of the harmonic oscillator. The black dashed lines are the classical sequences, while the solid curves correspond to the quantum case with values of $\hbar \in \{2^{-4}, 2^{-5}, 2^{-6}, 2^{-7}\}$ (light to dark).

The three figures clearly show that these quantities obey the correspondence principle: the difference between the quantum and classical Krylov complexities and Arnoldi sequences decrease in proportion with \hbar and the Krylov states become nearly identical.

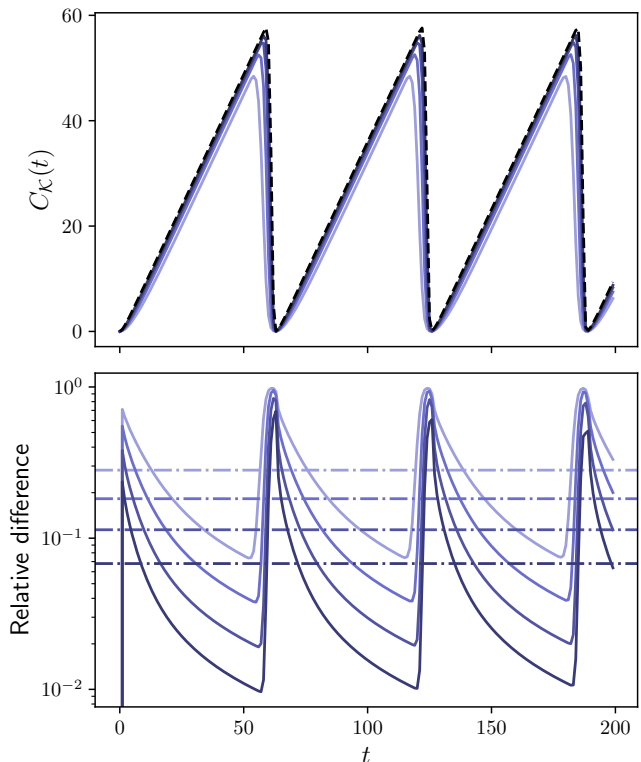


Figure 2. Quantum-to-classical correspondence in the Krylov complexity of the harmonic oscillator. Top panel: Krylov complexity as a function of time in the classical (black dashed line) and quantum (solid lines). Bottom panel: relative difference (to the classical) between the classical and quantum complexities (solid lines) and their average values (dash-dotted lines). The quantum curves correspond to values of $\hbar \in \{2^{-4}, 2^{-5}, 2^{-6}, 2^{-7}\}$ (light to dark).

It is noteworthy that in each period the complexity [Fig. 2] sets into a linear growth, indicating a ballistic propagation of the wavefunction β_{nt} in completely regular dynamics. The same growth is consistent with the profile of the Arnoldi sequences [Fig. 1], which in each period quickly set into $a_n \sim 0$, $b_n \sim 1$ and $c_n \sim 0$. In this regime Eq. (6) essentially becomes a transport equation, so the initial wave profile given by the autocorrelation β_{0t} is transported with unit speed, and thus the Krylov complexity grows as $C_{\mathcal{K}}(t) \sim t$. Such a regime is expected of chaotic dynamics [15, 31], although in that case it should last indefinitely, yielding a net mean growth in complexity, which highlights the need to study the long-time behavior of the Krylov complexity.

The structure of the Krylov states [Fig. 3] consists of a leading positive *head* and a decaying sign-alternating *tail*. These features are understood by the way the orthonor-

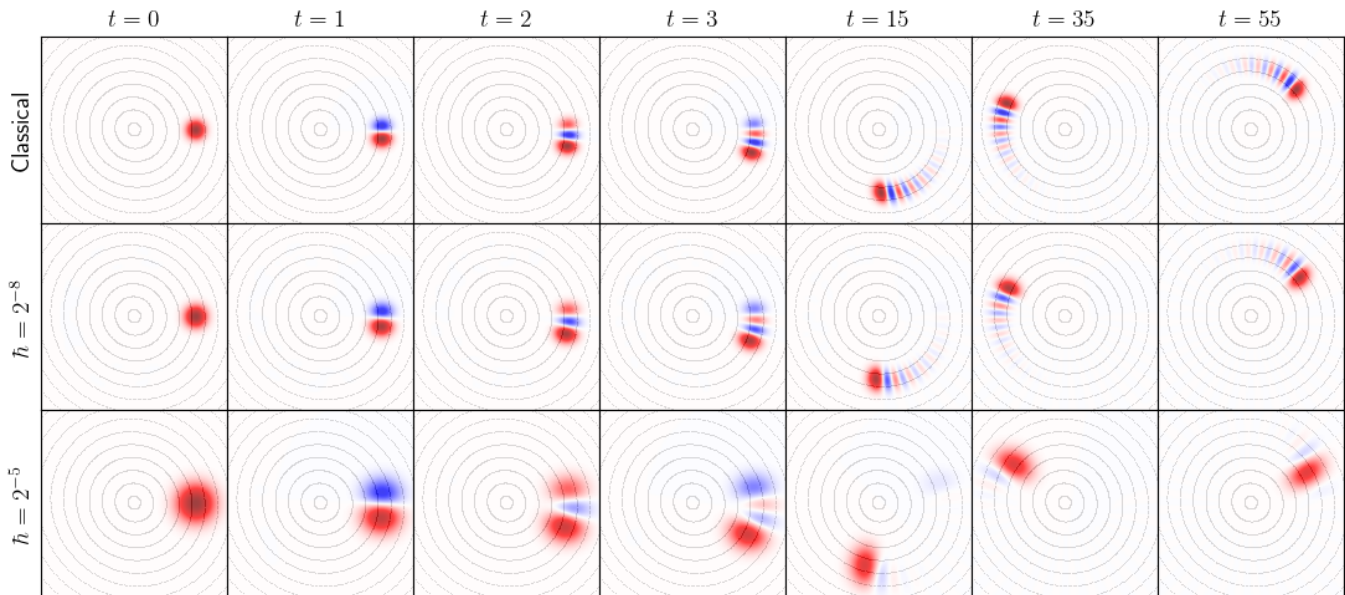


Figure 3. Classical and quantum phase space portraits of the Krylov states generated at various times t for the evolution of the harmonic oscillator. The quantum Krylov states are represented via the Husimi distribution. The colormap in each row is normalized with respect to its first Krylov state.

malization procedure works, which is simply to introduce negativities where the distributions overlap, and are not a particularity of this system but universal [See App. A]. This feature is also reflected in the initially alternating sequence c_n as they are the autocorrelation of the Krylov states (2).

The way in which the quantum Krylov states, as represented in phase-space by their Husimi distributions in Fig. 3, seem to simply be the classical Krylov states but for a distribution with a larger variance is deceiving. This is indeed the case for the first one as can be deduced from Eq. (22), but is not true in general. In App. C we show that simply matching the variance of the classical distribution to that of the Husimi won't lead to the same Krylov states nor complexity.

B. Harper map

We now turn to an example of a non-linear system exhibiting both integrable and chaotic behavior, although we will restrict the scope of this work to its regular regime with a weak non-linearity. The classical Harper map is defined on the unit square as

$$\begin{aligned} q' &= q - k \sin(2\pi p) \pmod{1} \\ p' &= p + k \sin(2\pi q') \pmod{1}. \end{aligned} \quad (23)$$

This system has a periodic phase space in both q and p directions, implying it is contained in the unit torus. Quantizing it leads to a Hilbert space of finite dimension N [30] requiring the consistency relation $2\pi\hbar N = 1$, such that the classical limit is obtained by taking $N \rightarrow \infty$.

This effectively discretizes the phase space in the sense that the \hat{q} and \hat{p} operators have a finite and discrete number of eigenstates $|q_n\rangle$ and $|p_n\rangle$, respectively. The periodicity is reflected in the fact that a unit translation of these states must contribute with, at most, a complex phase:

$$|q_n + 1\rangle = e^{i2\pi\bar{p}} |q_n\rangle, \quad |p_n + 1\rangle = e^{i2\pi\bar{q}} |p_n\rangle. \quad (24)$$

One then obtains the eigenvalues of the position and momentum operators as $q_n = \frac{n+\bar{q}}{N}$ and $p_n = \frac{n+\bar{p}}{N}$, respectively, for $n = 0, \dots, N-1$. These phases $\chi_q = 2\pi\bar{p}$ and $\chi_p = 2\pi\bar{q}$ are called Floquet phases. They specify different Hilbert spaces [32] and cannot be chosen trivially as they have an effect on the dynamics: an arbitrary choice can break symmetries present in the underlying classical map. See Ref. [29] for an example in another map defined on the unit torus, where some choices of Floquet phases would break its R-symmetry (reflection symmetry). The Harper map possesses both an R-symmetry and T-symmetry (time reversal symmetry), we have thus set $\bar{q} = 0.5$ and $\bar{p} = 0$ since we have observed numerically that such a choice preserves them. Its resulting quantum evolution is described by the Floquet unitary

$$U = e^{-iNk \cos(2\pi\bar{q})} e^{-iNk \cos(2\pi\bar{p})}. \quad (25)$$

The initial state here chosen is a classical Gaussian distribution as in Eq. (21), but with periodic boundary conditions to adapt it to the unit torus

$$\rho_0(q, p) = \frac{1}{2\pi\sigma^2} \sum_{n, m \in \mathbb{Z}} e^{-\frac{1}{2\sigma^2} [(q-q_0-n)^2 + (p-p_0-m)^2]}. \quad (26)$$

Analogously, its quantum counterpart is of the form (11). We study this model in its regular regime $k = 0.05$ with initial conditions $(q_0, p_0) = (0.4, 0.5)$ and $\sigma = 0.025$.

Figures 4, 5 and 6 show the quantum-to-classical correspondence of the Krylov complexity, the Arnoldi sequences and the Krylov states, respectively, as the dimension of the Hilbert space N increases. The observations made previously for the harmonic oscillator still generally hold, and at early times (or values of n) the quantities mentioned above behave quite similarly (as expected for the chosen initial state). In particular, a linear $C_{\mathcal{K}}(t) \sim t$ growth in the complexity within each cycle is also observed here. The differences lie in the lack of peri-

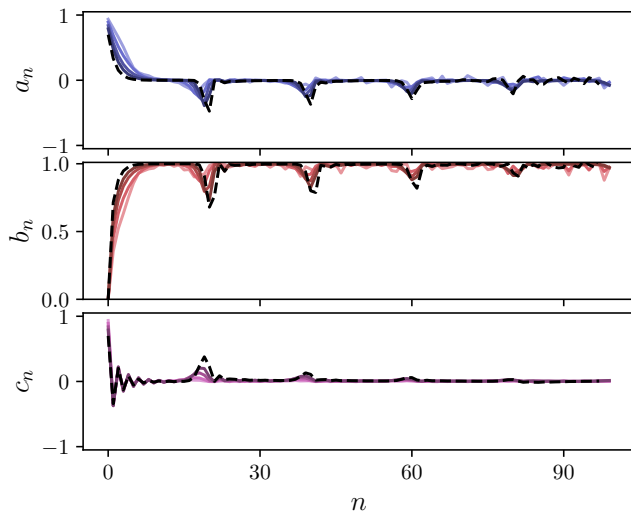


Figure 4. Quantum-to-classical correspondence in the Arnoldi sequences of the Harper map. The black dashed lines are the classical sequences, while the solid curves correspond to the quantum case with Hilbert space dimensions $N \in \{2^5, 2^6, 2^7, 2^8\}$ (light to dark).

odicity given by the non-linearity. As the distribution is pulled and stretched new Krylov states are always being generated to encode its changing geometry, which results in an additional net mean-growth of the complexity, and a decaying *reversion* of the Arnoldi sequences. These two observations are understood in view of Eq. (6): each revival of the autocorrelation emits a new wave packet from the origin that then propagates ballistically with unit speed. The oscillations in complexity eventually die out as the increasing amount of packets means the addition of another one is less impactful (due to normalization of the wavefunction) and the growth finally settles on a (purely) linear growth regime.

Another difference with respect to the oscillator is seen in that the quantum complexity is ultimately bounded, while the classical complexity seems to grow indefinitely. The quantum complexity is trivially bounded by the dimension of the operator Hilbert space. However, its dimension $\sim N^2$ is much larger than the saturation we observe in Fig. 5.

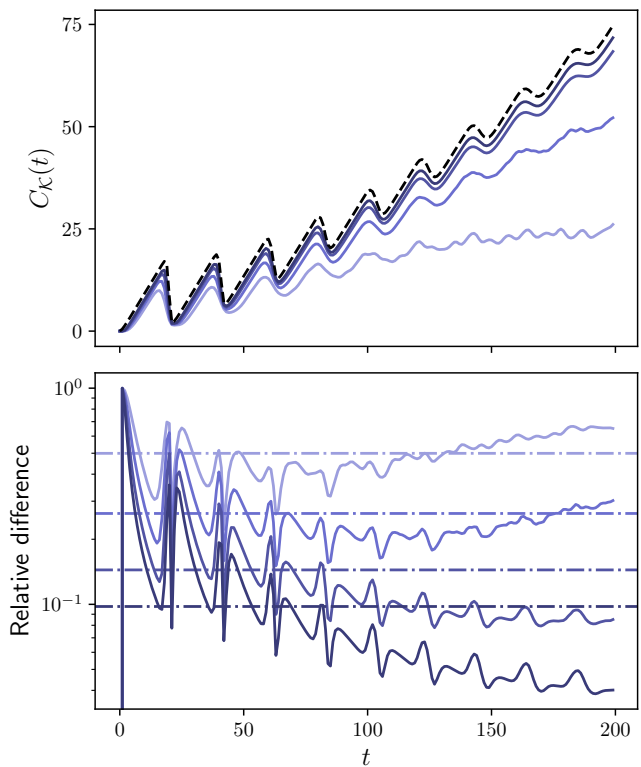


Figure 5. Quantum-to-classical correspondence in the Krylov complexity of the Harper map. Top panel: Krylov complexity as a function of time in the classical (black dashed line) and quantum (solid lines). Bottom panel: relative difference (to the classical) between the classical and quantum complexities (solid lines) and their average values (dash-dotted lines). The quantum curves correspond to Hilbert space dimensions $N \in \{2^5, 2^6, 2^7, 2^8\}$ (light to dark).

IV. FINAL REMARKS AND CONCLUSIONS

So far, most studies on complexity from the Krylov perspective have focused in autonomous systems that admit a Liouvillian representation and in the quantum or semi-classical regime, although the method can equally be applied to a classical evolution. By contrast, in this paper we focused in dynamics prescribed by a unitary (super)operator and defined a construction for the Krylov space of a purely classical evolution and of a quantum operator such that, through a phase-space representation via a quasiprobability distribution, we could explicitly demonstrate that the former is obtained as the classical limit of the latter after suitable choices of initial state and inner product are made. In this sense, the quantum and classical Krylov spaces thus defined obey the correspondence principle, and by extension so do the complexity and states.

The Krylov states show a universal structure composed of a positive leading term and a sign-alternating tail. The time evolution of the Krylov complexity is understood in terms of the phase-space representation of the Krylov

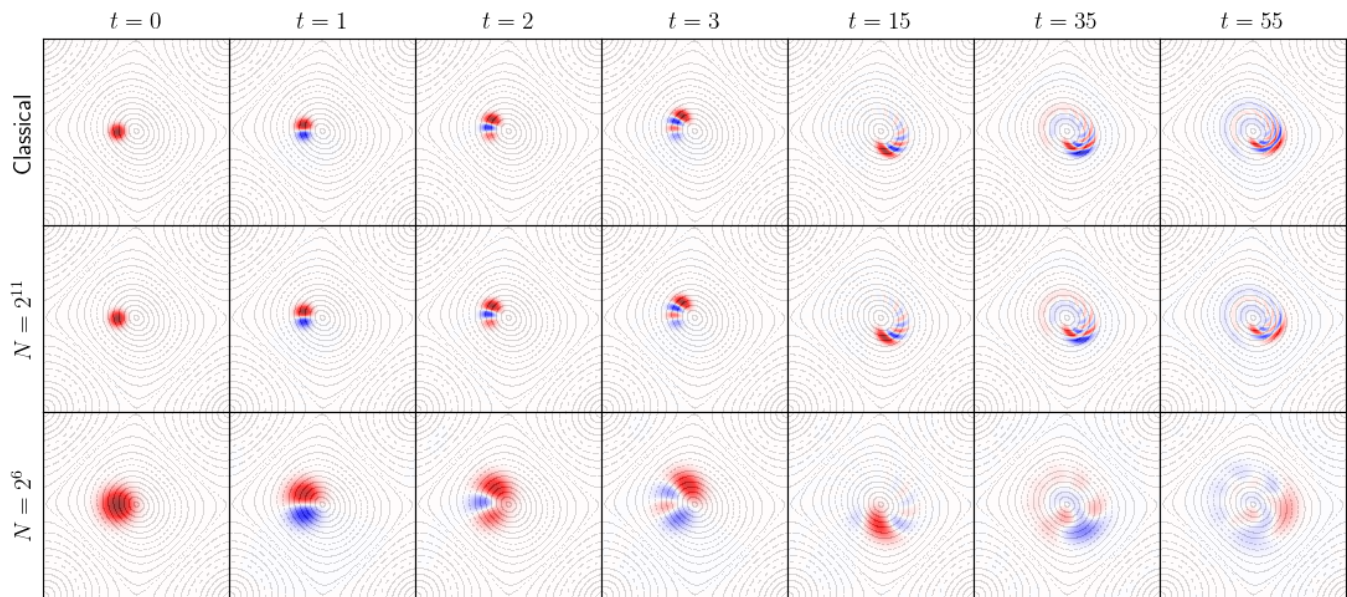


Figure 6. Classical and quantum phase space portraits of the Krylov states generated at various times t for the evolution of the Harper map. The quantum Krylov states are represented via the Husimi distribution. The colormap in each row is normalized with respect to its first Krylov state.

states. The complexity grows linearly as long as new ones are being generated, with oscillations that naturally arise from recursions, affecting its mean growth. While the classical complexity can in principle grow indefinitely even in a bounded evolution, we see that the quantum complexity is ultimately capped at a value much lower than the trivial bound given by the dimension of the operator Hilbert space. Remarkably, the classical complexity seems to upper-bound the quantum in the examples presented.

We have also explored alternative methods in which one could try to construct the classical Krylov space in correspondence with a given quantum Krylov space, in particular by matching the classical distribution to the phase-space representation of the quantum state, be it described by a pure density matrix or a ket. The failure of these alternative methods is understood in terms of the structural differences in the resulting Krylov states: those generated in the evolution of the pure density matrices have suppressed tails which reflects in a Krylov complexity larger than the classical, while those of the ket seem to scape the torus altogether, leading to a saturation of the complexity.

The focus of this paper was put to the study of the quantum-to-classical correspondence, the structure of the Krylov states as phase-space quantities and the subsequent understanding of Krylov complexity from such a perspective. For the sake of simplicity we restricted our examples to linear and weakly-non-linear systems in the vicinity of a fixed point. Extensions of these results into higher-dimensional, strongly non-linear or even chaotic systems are readily in reach. Although in the latter

cases numerical computation of the classical inner products provide a challenge since the distributions involved attain an arbitrarily complex structure. However, the general goal of this study was to provide a platform from which to ground the notions of complexity and ergodicity of unitary evolution, as understood from the Krylov perspective, in terms of well-understood notions in classical dynamics. In this regard, we believe this paper to constitute a first step in that direction.

V. ACKNOWLEDGMENTS

This work has been partially supported by CONICET (Grant No. PIP 11220200100568CO), UBACyT (Grant No. 20020220300049BA).

Appendix A: Krylov space from Gram-Schmidt procedure

Krylov space can equally be constructed from a direct Gram-Schmidt procedure as well as the Arnoldi iteration (1) mentioned in the main text. In this appendix we cast the results of the construction in terms of the former.

Once defined an inner product $(\cdot|\cdot)$ and induced norm $\|\cdot\| = \sqrt{(\cdot|\cdot)}$, we start with the normalized temporal series $\{\rho_0, \rho_1, \dots\}$. Then, in terms of the Gram-Schmidt procedure, the iteration reads

$$B_n \kappa_n = \rho_n - \sum_{l=0}^{n-1} (\kappa_l | \rho_n) \kappa_l. \quad (\text{A1})$$

Let G_n be the n -th Gram matrix defined as $(G_n)_{ij} = (\rho_i|\rho_j)$ with $i, j = 0, \dots, n$ (G_n is a $(n+1) \times (n+1)$ matrix). In this context, and for the inner products (7) and (9) considered, it is a symmetric correlation matrix $(G_n)_{ij} = c_{|j-i|} = (\rho_i|\rho_j)$. The result of the iteration can then be expressed in terms of its determinants $D_n = \det(G_n)$ as the Laplace expansion

$$\kappa_n = \sum_{t=0}^n (-1)^{t+n} \frac{D_{n-1}^{(t)}}{\sqrt{D_n D_{n-1}}} \rho_t, \quad (\text{A2})$$

where $D_{n-1}^{(t)}$ is the determinant of G_n with its last row and its t -th column removed. Since the Gram matrix is a correlation matrix, it is positive-definite and all of its determinants are positive. Then Eq. (A2) implies the oscillatory nature of the Krylov states seen in the main text [Figs. 3 and 6]. By comparison with Eq. (4) it directly follows that

$$\alpha_{tn} = (-1)^{t+n} \frac{D_{n-1}^{(t)}}{\sqrt{D_n D_{n-1}}} \quad (\text{A3})$$

and then

$$\beta_{nt} = \sum_{s=0}^n (-1)^{n+s} \frac{D_{n-1}^{(s)}}{\sqrt{D_n D_{n-1}}} c_{t-s}. \quad (\text{A4})$$

Further, from (A1) and (A4) it is easy to see that

$$B_n = \beta_{nn} = \frac{1}{\alpha_{nn}} = \sqrt{\frac{D_n}{D_{n-1}}} > 0. \quad (\text{A5})$$

On the other hand, one can deduce from the Arnoldi iteration that $\beta_{nn} = \prod_{i=1}^n b_i$, which relates the sequences B_n and b_n .

Appendix B: Semiclassical evolution of the P-distribution

The quantum-to-classical correspondence argued relies on the fact that the P-distribution of the evolved quantum state asymptotically amounts to the classical evolution of the distribution itself in the semiclassical limit, as Eq. (17) expresses [23]:

$$P_{U\rho}(x) \approx P_\rho(\mathcal{M}^{-1}(x)) \equiv \mathcal{P}P_\rho(x). \quad (\text{B1})$$

Here we provide proof of this fact for a general class of quantized classical maps.

Instead of calculating $P_{U\rho}(x)$ directly, we will make use of the Husimi distribution

$$H_\rho(z) = \frac{1}{2\pi\hbar} \langle \alpha(z) | \hat{\rho} | \alpha(z) \rangle \quad (\text{B2})$$

and utilize how these two representations relate in the semiclassical limit, as follows. Recall that the P-representation allows one to expand the density matrix in a ‘‘diagonal’’ form as

$$\hat{\rho} = \int dx P_\rho(x) |\alpha(x)\rangle \langle \alpha(x)|, \quad (\text{B3})$$

such that by inserting this expression into Eq. (B2) and taking the semiclassical limit (provided it exists) one gets

$$H_\rho(z) = \frac{1}{2\pi\hbar} \int dx P_\rho(x) |\langle \beta(x) | \alpha(z) \rangle|^2 \approx P_\rho(z), \quad (\text{B4})$$

where we have used that the overlap between coherent states is $|\langle \beta(x) | \alpha(z) \rangle|^2 = e^{-\frac{1}{2\hbar}(z-x)^2}$ and that the 0-variance limit of a Gaussian distribution is a Dirac delta. This allows us to compute $H_{U\rho}(x)$ instead of $P_{U\rho}(x)$, which is a more straight-forward calculation.

Now the problem is shifted to that of calculating the semiclassical limit of

$$\begin{aligned} H_{U\rho}(z) &= \frac{1}{2\pi\hbar} \langle \alpha(z) | U \hat{\rho} U^\dagger | \alpha(z) \rangle \\ &= \frac{1}{2\pi\hbar} \int dw P_\rho(w) |\langle \beta(w) | U^\dagger | \alpha(z) \rangle|^2, \end{aligned} \quad (\text{B5})$$

where the last equality is obtained again using the P-representation for $\hat{\rho}$. The utility of using the Husimi and P-distributions in such a way is that it reduces the problem to that of evaluating $\langle \beta(w) | U^\dagger | \alpha(z) \rangle$ semiclassically. The semiclassical propagation of coherent states is a topic treated rigorously and quite generally in Ref. [24]. In this appendix we provide an alternative and clear result by calculating how coherent states are propagated in the semiclassical limit directly. The essential result is that a coherent state is evolved semiclassically into a *squeezed* coherent state centred on the trajectory of the classical evolution up to an $O(\sqrt{\hbar})$ correction. As we will see, this is so because for sufficiently small values of \hbar the Gaussian packet is localized enough that, while it is transported by the *full* classical map, only the *linearized* classical map is involved in its deformation. This means that the Gaussian packet evolves into another Gaussian packet, although squeezed, with a variance proportional to \hbar . As a result, the overlap in Eq. (B5) will localize the integral at the next point in the classical trajectory in the semiclassical limit.

Consider a time-dependent delta-kicked system with the Hamiltonian

$$H(q, p, t) = f(q) + g(p) \sum_{n \in \mathbb{Z}} \delta(t - n). \quad (\text{B6})$$

Its stroboscopic evolution is obtained by integrating the Hamilton equations from just after one kick to just after the next one $t \in [n + \delta, n + 1 + \delta]$ with $\delta \rightarrow 0^+$, which defines the classical map $(q', p') = \mathcal{M}(q, p)$ through

$$\begin{aligned} q' &= q + g'(p) \\ p' &= p - f'(q'). \end{aligned} \quad (\text{B7})$$

The corresponding quantum map can be obtained by canonical quantization of (B6) and calculation of the evolution operator for that same stroboscopic evolution (the Floquet operator)

$$U = e^{-\frac{i}{\hbar} f(\hat{q})} e^{-\frac{i}{\hbar} g(\hat{p})}. \quad (\text{B8})$$

Let $z = (q, p)$, given a coherent state $|\alpha\rangle$ with $\alpha = (q + ip)/\sqrt{2\hbar}$ we will calculate the semiclassical expansion of $U^\dagger|\alpha\rangle$ in the position representation $|y\rangle$. By inserting momentum and position identities $\mathbb{I} = \int d\xi |\xi\rangle\langle\xi|$, $\mathbb{I} = \int dx |x\rangle\langle x|$ before and after U^\dagger , respectively, one gets

$$\langle y|U^\dagger|\alpha\rangle = \frac{1}{\sqrt{2(\pi\hbar)^{3/2}}} \int d\xi e^{\frac{i}{\hbar}(g(\xi)+\xi y)} I_x(\xi), \quad (\text{B9})$$

where

$$I_x(\xi) = \frac{1}{\sqrt{2\pi\hbar}} \int dx e^{\frac{i}{\hbar}\phi(x,\xi)} e^{-\frac{1}{2\hbar}(x-q)^2}, \quad (\text{B10})$$

with $\phi(x, \xi) = f(x) - \xi x + px$. The Gaussian factor localizes the integrand around q , which we can make explicit through a change of variables $x = q + \sqrt{\hbar}u$. Expanding the phase in powers of \hbar : $\phi(x, \xi) = f(q) - \xi q + pq + \sqrt{\hbar}u(f'(q) - \xi + p) + 1/2f''(q)\hbar u^2 + O(\hbar^{3/2})$, we can ignore higher order terms since they amount to an additive $O(\sqrt{\hbar})$ correction to I_x . Replacing this expansion back into (B10) with the change of variables yields

$$I_x(\xi) = \frac{1}{\sqrt{2\pi}} e^{\frac{i}{\hbar}(f(q)-\xi q+pq)} \int du e^{\frac{i}{\sqrt{\hbar}}(f'(q)-\xi+p)u} \times e^{-\frac{1}{2}(1-if''(q))u^2} + O(\sqrt{\hbar}) \quad (\text{B11})$$

The remaining integral is the Fourier transform of a Gaussian evaluated at $(f'(q) - \xi + p)/\sqrt{\hbar}$, so we finally get

$$I_x(\xi) = \frac{1}{\sqrt{1-if''(q)}} e^{\frac{i}{\hbar}(f(q)+pq)} e^{-\frac{1}{2\hbar} \frac{(\xi-p-f'(q))^2}{1-if''(q)}} + O(\sqrt{\hbar}). \quad (\text{B12})$$

Inserting this back into Eq. (B9) yields

$$\langle y|U^\dagger|\alpha\rangle = \frac{e^{\frac{i}{\hbar}(f(q)+pq)}}{(\pi\hbar)^{1/4} \sqrt{1-if''(q)}} I_\xi(y) + O(\sqrt{\hbar}), \quad (\text{B13})$$

where

$$I_\xi(y) = \frac{1}{\sqrt{2\pi\hbar}} \int d\xi e^{\frac{i}{\hbar}(g(\xi)+\xi y-\xi q)} e^{-\frac{1}{2\hbar} \frac{(\xi-p-f'(q))^2}{1-if''(q)}}. \quad (\text{B14})$$

Much like before, this integral is localized by the Gaussian (the part with real quadratic exponent), and a completely analogous procedure can be utilized to calculate it. Together with the previous expansion of f , this amounts to considering only up to quadratic terms in the Hamiltonian (B6), or the linearized version of the map (B7). The result reads

$$I_\xi(y) = \frac{\sqrt{1+i\delta}}{|\sigma|} e^{\frac{i}{\hbar}\varphi_U(\alpha)} e^{-\frac{1}{2\hbar} \frac{1+i\delta}{|\sigma|^2}(y-q')^2} e^{\frac{i}{\hbar}p'y} + O(\sqrt{\hbar}), \quad (\text{B15})$$

where we have defined $\sigma = 1 - g''f'' + ig''$, $\delta = g'' - f'' + g''f''$ and $\varphi_U(\alpha) = f + pq + g - p'q$ is a phase dependent on the coherent state and the map, where $p' \equiv p + f'(q)$,

$q' \equiv q - g'(p')$. In all the previous expressions f and its derivatives are evaluated at q , and g and its derivatives are evaluated at p' . Putting it all together we finally get

$$\langle y|U^\dagger|\alpha\rangle = \frac{\sqrt{\sigma}}{|\sigma|} \frac{e^{\frac{i}{\hbar}\varphi_U(\alpha)}}{(\pi\hbar)^{1/4}} e^{-\frac{1}{2\hbar} \frac{1+i\delta}{|\sigma|^2}(y-q')^2} e^{\frac{i}{\hbar}p'y} + O(\sqrt{\hbar}). \quad (\text{B16})$$

We have thus obtained that a coherent state localized at a point $z = (q, p)$ is evolved in one step of the inversed quantum map (B8) into a *squeezed* coherent state centred at a point $z' = (q', p')$ given by the inverse of the classical map (B7) \mathcal{M}^{-1} as

$$\begin{aligned} p' &= p + f'(q) \\ q' &= q - g'(p'), \end{aligned} \quad (\text{B17})$$

with a squeezing determined by the second derivatives at that point $f''(q)$, $g''(p')$, up to an $O(\sqrt{\hbar})$ correction. From now on we drop the O notation and switch to the notation \approx denoting the lowest-order term in powers of \hbar .

All that's left is to compute the projection onto another coherent state $\langle\beta|U^\dagger|\alpha\rangle$ with $\beta(w) = (x + i\xi)/\sqrt{2\hbar}$ and $w = (x, \xi)$, which is tedious but straightforward: insert a position identity $\mathbb{I} = \int dy |y\rangle\langle y|$ after $\langle\beta|$, use Eq. (B16), expand each quadratic term in y inside the exponentials and complete the squares; the remaining integral will be the Fourier transform of a Gaussian. Rearranging things carefully, the result is

$$\langle\beta|U^\dagger|\alpha\rangle \approx \sqrt{\frac{2\sigma}{|\sigma|^2 + 1 + i\delta}} e^{\frac{i}{\hbar}(\varphi_U(\alpha) - \vartheta_U(\beta, \alpha))} \times e^{-\frac{1}{4\hbar}(w-z')\mathbb{V}^{-1}(w-z')^t}, \quad (\text{B18})$$

with the additional phase

$$\begin{aligned} \vartheta_U(\beta, \alpha) &= \frac{1}{(|\sigma|^2 + 1)^2 + \delta^2} \left\{ \frac{1}{2} |\sigma|^2 \delta \left[(x-q')^2 - (\xi-p')^2 \right] \right. \\ &\quad \left. + (\xi - p') \left[|\sigma|^2 (|\sigma|^2 + 1)x + (|\sigma|^2 + 1 + \delta^2)q' \right] \right\}, \end{aligned}$$

where the covariance matrix is

$$\mathbb{V}^{-1} = \frac{2}{(|\sigma|^2 + 1)^2 + \delta^2} \begin{pmatrix} |\sigma|^2 + 1 + \delta^2 & -|\sigma|^2 \delta \\ -|\sigma|^2 \delta & |\sigma|^2 (|\sigma|^2 + 1) \end{pmatrix}, \quad (\text{B19})$$

which is a proper non-singular and positive-definite matrix for all values of f'' , g'' with determinant $\det(\mathbb{V}^{-1}) = 4|\sigma|^2 / [(|\sigma|^2 + 1)^2 + \delta^2]$. Finally, we obtain

$$\frac{1}{2\pi\hbar} |\langle\beta(w)|U^\dagger|\alpha\rangle|^2 \approx \frac{1}{2\pi\hbar \sqrt{\det(\mathbb{V})}} e^{-\frac{1}{2\hbar}(w-z')\mathbb{V}^{-1}(w-z')^t}, \quad (\text{B20})$$

a 2D Gaussian distribution. By diagonalizing $\mathbb{V} = U^{-1}\mathbb{D}U$ (where U is an orthogonal matrix) and changing variables $\zeta = (w - z')U$ (note that $d\zeta = dw$ since

$\det(U) = 1$) this can be rewritten as two separate, independent 1D Gaussian distributions, each with zero mean and variance directly proportional to \hbar :

$$\frac{1}{2\pi\hbar} |\langle \beta(\zeta U^{-1} + z') | U^\dagger | \alpha \rangle|^2 \approx \mathcal{N}(u|0, \hbar\lambda_1) \mathcal{N}(v|0, \hbar\lambda_2),$$

where λ_1 and λ_2 are \mathbb{V} 's eigenvalues and $\zeta = (u, v)$. The 0-variance limit of a Gaussian distribution is a Dirac delta, so taking the $\hbar \rightarrow 0$ limit yields

$$\frac{1}{2\pi\hbar} |\langle \beta(\zeta U^{-1} + z') | U^\dagger | \alpha \rangle|^2 \approx \delta(u)\delta(v) = \delta(\zeta),$$

and changing back to the original variables we finally arrive at

$$\frac{1}{2\pi\hbar} |\langle \beta(w) | U^\dagger | \alpha(z) \rangle|^2 \approx \delta(w - \mathcal{M}^{-1}(z)), \quad (\text{B21})$$

after using that $\delta(zU) = \delta(z)/\det(U) = \delta(z)$ for any z , and recalling that $z' = \mathcal{M}^{-1}(z)$ [Eq. (B17)]. Replacing Eq. (B21) into Eq. (B5):

$$H_{U\rho}(z) \approx P_\rho(\mathcal{M}^{-1}(z)).$$

Finally, Eq. (B4) allows us to write

$$P_{U\rho}(z) \approx P_\rho(\mathcal{M}^{-1}(z)) \equiv \mathcal{P}P_\rho(z), \quad (\text{B22})$$

where we have used the definition of the Perron-Frobenius operator [Eq. (8)].

This calculation was carried out for a single application of the map, and we don't prove the more general statement

$$P_{U^t\rho}(z) \approx \mathcal{P}^t P_\rho(z).$$

At a fixed value of \hbar , this will hold for as long as there is a semiclassical correspondence, which is the Ehrenfest time $t \leq \tau_E$. This timescale is controlled by the stability of the classical trajectory such that $\tau_E \sim 1/\hbar^{1/2}$ for a stable trajectory and $\tau_E \sim \log(\hbar)$ for an unstable one.

As a final note, we haven't considered maps defined on the torus for this calculation, but since for small enough values of \hbar (large enough values of N , the dimension of the Hilbert space for the quantized torus) the discrepancies become vanishingly small, the same result holds.

Appendix C: Lack of correspondence with alternative methods

In the main text we see quantum-to-classical correspondence of the Arnoldi procedure, and thus of the Krylov states and complexity, for the von Neumann evolution of a density matrix. This is, its quantum Krylov space converges to the purely classical Krylov space for the distribution that defines its Glauber-Sudarshan P-representation (11). One alternative approach may be to apply the Arnoldi iteration to the evolution of a pure

density matrix $|\alpha(x)\rangle\langle\alpha(x)|$ or even a ket $|\alpha(x)\rangle$. In both cases, the corresponding Husimi distribution is a Gaussian centred at the point $x = (q, p)$ with variance $\sigma^2 = \hbar$. Thus in the classical limit $\hbar \rightarrow 0$ one may expect the result to match that of the classical evolution of the same Gaussian distribution for sufficiently small timescales [25–27]. In this appendix we point out that this is not a viable alternative in the current context.

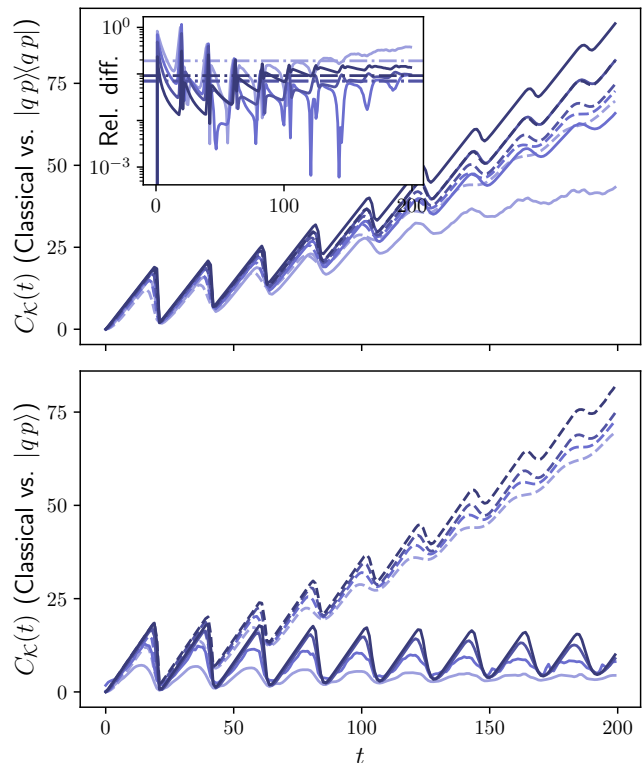


Figure 7. Comparison of the Krylov complexity for the quantum evolution of a pure coherent-state density matrix (top, solid lines), a coherent state (bottom, solid lines) and the classical (dashed lines) evolution of a Gaussian distribution with variance $\sigma^2 = \hbar = 1/2\pi N$ for the Harper map, with $N \in \{2^6, 2^7, 2^8, 2^9\}$ (light to dark). The inset shows the relative difference (to the classical) between the classical and quantum complexities (solid lines) and their average values (dash-dotted lines). Here $|q, p\rangle \equiv |\alpha(q, p)\rangle$.

In Fig. 7 we show comparisons between the Krylov complexity obtained for the evolution of an initially pure coherent-state density matrix, a coherent state, and a classical Gaussian distribution with variance $\sigma^2 = \hbar$, as discussed just above, for the Harper map. Figure 8 shows some of the corresponding Krylov states. Aside from the variance, all other parameters have been kept the same as in the main text. The Krylov complexity for the coherent state is completely different to the classical (note that the Krylov complexity of states is also referred to as the spread complexity), and while that of the density matrix does fare better, there is no clear correspondence. In fact, the average relative difference between the quantum and

classical *increases* with a decrease in \hbar when going from $N = 2^8$ to $N = 2^9$ [Fig. 7].

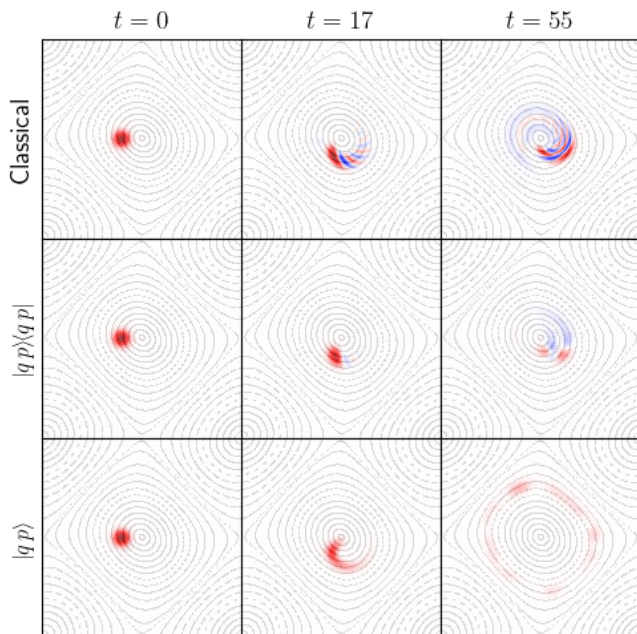


Figure 8. Comparison of the Krylov states generated at various times t for the quantum evolution of a pure coherent density matrix, a coherent state and the classical evolution of a Gaussian distribution with variance $\sigma^2 = \hbar = 1/2\pi N$ for the Harper map, with $N = 2^8$. The colormap in each row is normalized with respect to its first Krylov state. Here $|q, p\rangle \equiv |\alpha(q, p)\rangle$.

Compared to those of the classical evolution, the states

generated by the density matrix are only quantitatively different, while those of the state are also *qualitatively* different, having a distinct structure altogether [Fig. 8]. One may expect the latter two to show some structural differences since one is an operator Krylov space constructed from the propagator \mathcal{U} , and the other a state space from the usual unitary evolution operator U . The space of density matrices is not closed upon the operations carried out in the Arnoldi iteration, and as a result the initially pure state generates Krylov states that are not pure. On the other hand, the space of kets *is* closed, so pure states remain pure, and the Husimi distributions of the resulting Krylov states are by necessity positive. These two observations encapsulate why the Krylov state of the pure density matrix is not equivalent to that of the ket.

The aforementioned differences in the complexities can be interpreted from the distinct features of the generated Krylov states. The states generated by the pure density matrix have suppressed tails (compared to the classical) meaning most of the weight in (4) is set on the coefficient accompanying ρ_n , which in turn implies a large overlap ($\kappa_n|\rho_t \equiv \beta_{nt}$ for $n \approx t$, and as a result the Krylov complexity (10) is consistently higher for the pure density matrix as seen in Fig. 7. One striking feature of the Krylov states generated by the coherent state $|\alpha(x)\rangle$ is that beyond the first period $T \sim 25$ they are localized *outside* the torus [See Fig. 8]. Because after the period the newly generated states lie beyond the torus, the evolution has little overlap with them $\beta_{nt} \sim 0$ for $n \gtrsim T$ and the wavefunction is confined to the interval $n \in [0, T]$. The oscillations in the Krylov complexity decay, and it settles into a value $C_{\mathcal{K}} \sim T/2$ as the wavefunction becomes uniform in that interval.

-
- [1] O. Bohigas, M. J. Giannoni, and C. Schmit, Characterization of chaotic quantum spectra and universality of level fluctuation laws, *Phys. Rev. Lett.* **52**, 1 (1984).
- [2] F. Haake, *Quantum signatures of chaos* (Springer, 1991).
- [3] M. L. Mehta, *Random matrices* (Elsevier, 2004).
- [4] S. Wimberger, *Nonlinear dynamics and quantum chaos*, Vol. 10 (Springer, 2014).
- [5] F. Haake and K. Życzkowski, Random-matrix theory and eigenmodes of dynamical systems, *Phys. Rev. A* **42**, 1013 (1990).
- [6] M. Kus, J. Mostowski, and F. Haake, Universality of eigenvector statistics of kicked tops of different symmetries, *Journal of Physics A: Mathematical and General* **21**, L1073 (1988).
- [7] F. M. Izrailev, Chaotic structure of eigenfunctions in systems with maximal quantum chaos, *Physics Letters A* **125**, 250 (1987).
- [8] A. Goussev, R. A. Jalabert, H. M. Pastawski, and D. A. Wisniacki, Loschmidt echo, *Scholarpedia* **7**, 11687 (2012).
- [9] R. A. Jalabert and H. M. Pastawski, Environment-independent decoherence rate in classically chaotic systems, *Phys. Rev. Lett.* **86**, 2490 (2001).
- [10] S. H. Shenker and D. Stanford, Stringy effects in scrambling, *Journal of High Energy Physics* **2015**, 1 (2015).
- [11] B. Swingle, Unscrambling the physics of out-of-time-order correlators, *Nature Physics* **14**, 988 (2018).
- [12] T. Notenson, I. García-Mata, A. J. Roncaglia, and D. A. Wisniacki, Classical approach to equilibrium of out-of-time ordered correlators in mixed systems, *Physical Review E* **107**, 064207 (2023).
- [13] I. García-Mata, M. Saraceno, R. A. Jalabert, A. J. Roncaglia, and D. A. Wisniacki, Chaos signatures in the short and long time behavior of the out-of-time ordered correlator, *Phys. Rev. Lett.* **121**, 210601 (2018).
- [14] D. E. Parker, X. Cao, A. Avdoshkin, T. Scaffidi, and E. Altman, A universal operator growth hypothesis, *Phys. Rev. X* **9**, 041017 (2019).
- [15] P. Suchsland, R. Moessner, and P. W. Claeys, Krylov complexity and trotter transitions in unitary circuit dynamics, *Phys. Rev. B* **111**, 014309 (2025).
- [16] V. Viswanath and G. Müller, *The recursion method: application to many-body dynamics*, Vol. 23 (Springer Science & Business Media, 2008).

- [17] E. Rabinovici, A. Sánchez-Garrido, R. Shir, and J. Sonner, Operator complexity: a journey to the edge of krylov space, *J. High Energy Phys.* **2021** (6).
- [18] V. Balasubramanian, P. Caputa, J. M. Magan, and Q. Wu, Quantum chaos and the complexity of spread of states, *Phys. Rev. D* **106**, 046007 (2022).
- [19] A. A. Nizami and A. W. Shrestha, Spread complexity and quantum chaos for periodically driven spin chains, *Phys. Rev. E* **110**, 034201 (2024).
- [20] R. J. Glauber, Coherent and incoherent states of the radiation field, *Phys. Rev.* **131**, 2766 (1963).
- [21] E. C. G. Sudarshan, Equivalence of semiclassical and quantum mechanical descriptions of statistical light beams, *Phys. Rev. Lett.* **10**, 277 (1963).
- [22] L. Mandel and E. Wolf, *Optical Coherence and Quantum Optics* (Cambridge University Press, 1995).
- [23] We denote by $X \approx Y$ that Y is the lowest-order term in the asymptotical expansion of X in terms of \hbar .
- [24] D. Robert and M. Combescure, *Coherent states and applications in mathematical physics* (Springer, 2021).
- [25] F. Toscano, R. L. de Matos Filho, and L. Davidovich, Decoherence and the quantum-classical limit in the presence of chaos, *Phys. Rev. A* **71**, 010101 (2005).
- [26] D. A. Wisniacki and F. Toscano, Scaling laws in the quantum-to-classical transition in chaotic systems, *Phys. Rev. E* **79**, 025203 (2009).
- [27] Z. P. Karkuszewski, J. Zakrzewski, and W. H. Zurek, Breakdown of correspondence in chaotic systems: Ehrenfest versus localization times, *Phys. Rev. A* **65**, 042113 (2002).
- [28] K. Husimi, Some formal properties of the density matrix, *Proceedings of the Physico-Mathematical Society of Japan. 3rd Series* **22**, 264 (1940).
- [29] M. Saraceno, Classical structures in the quantized baker transformation, *Annals of Physics* **199**, 37 (1990).
- [30] P. Leboeuf and A. Voros, Chaos-revealing multiplicative representation of quantum eigenstates, *Journal of Physics A: Mathematical and General* **23**, 1765 (1990).
- [31] G. F. Scialchi, A. J. Roncaglia, C. Pineda, and D. A. Wisniacki, Exploring quantum ergodicity of unitary evolution through the krylov approach, *Phys. Rev. E* **111**, 014220 (2025).
- [32] P. Bianucci, J. P. Paz, and M. Saraceno, Decoherence for classically chaotic quantum maps, *Phys. Rev. E* **65**, 046226 (2002).